Using Lidar Data to Predict Photo Interpreted Attributes

Miles Elliot LeFevre

A thesis

Submitted in partial fulfillment of the

requirements for the degree of

Masters of Science

University of Washington

2018

Committee:

Jerry F. Franklin

Van R. Kane

Derek J. Churchill

L. Monika Moskal

Program Authorized to Offer Degree:

School of Environmental and Forest Sciences

University of Washington

Abstract

Using Lidar Data to Predict Photo Interpreted Attributes

Miles Elliot LeFevre

Chair of the Supervisory Committee:
Professor Jerry F. Franklin
School of Environmental and Forest Sciences

Large datasets and robust workflows exist for both the photo interpretation and Lidar methodologies. Both methodologies have unique and non-overlapping strengths in describing forest conditions. Bridging the data products of these methodologies would expand the capabilities for both approaches. To my knowledge no previous studies have attempted to evaluate the comparability of photo interpretation datasets and Lidar data products. In this study I attempted to develop methods that incorporate Lidar products into the photo interpretation process, and evaluate the comparability of Lidar products to photo interpretation attributes. I evaluated correlations between photo interpretation attributes and logical analog Lidar data products. I developed models to predict photo interpretation attributes using Lidar data products and predictor variables. I summarized photo interpretation attributes and equivalent Lidar predicted attributes using watershed scale spatial pattern metrics to evaluate the substitutability of the datasets in a mid-scale analysis scenario. Models of photo interpretation attributes describing Overstory Canopy Cover performed better than those describing characteristics of Understory Canopy Cover. Models performed poorly in exact matching of photo interpretation classification, but frequently predicted classes within one class of observed values for ordinal metrics. Comparisons of watershed scale summary metrics produced mixed results.

Table of Contents

1. Introduction

The pace and scale of forest restoration is increasing in the Pacific Northwest region (Noss 2001; Churchill et al. 2013). These forest management efforts are shifting towards a holistic, landscape scale approach (Hessburg et al. 2015). Land managers are challenged to adapt well established stand scale techniques to broader spatial extent frameworks (Lertzman and Fall 1998; Kane et al. 2010a). These shifts in focus create a clear need for remote sensing solutions in characterizing forest land conditions at a watershed and regional grain.

Two remote sensing approaches commonly used in forest management are photo interpretation and Light Detection and Ranging (Lidar). Both approaches have unique advantages and limitations. The scope of utility for each methodology is defined by its approach and application.

Photo interpretation is widely used as a landscape evaluation tool (Hessburg et al. 1999a; Cosco 2011). Photo interpretation is defined as the identification and description of objects in photos (Avery 1969). This broad definition is highly inclusive. For the purposes of modern photo interpretation in the application of remote sensing of forested areas, I will define photo interpretation as the delineation and characterization of forest structural and compositional conditions using stereoscopic areal images.

The practice of photo interpretation began shortly after the advent of the photograph in 1827 (Baker et al. 1997). Photogrammetry, which is a methodology that was a predecessor to photo interpretation, was first employed in the 1850's as reconnaissance research for the French Army (Avery 1969). Aerial photographs were first used to survey forest conditions in 1919 by the Laurentide paper Company in Quebec (Baker et al. 1997). The U.S. Forest Service (USFS) first began using aerial photo interpretation in timber type-mapping on the national forests in the 1930's (Avery 1969). Since then photo interpretation has grown to become a common remote sensing approach to characterizing forest conditions.

Although the technology of image collection and stereoscopic viewing has improved, the practice of photo interpretation remains relatively unchanged (Spurr 1960). A photo interpreter viewing an aerial image of forested area will delineate the photo into patches of essentially homogeneous forest conditions for the attributes of interest. The photo interpreter will then ascribe the attributes as they appear in the photo for each patch. Long established elements of photo interpretation are relationships between the attributes of interest on the ground and the corresponding variation in tone, color, geometry, and spatial arrangements of their representation in imagery (Baker et al. 1997). Specific protocols of photo interpretation are often developed to suit the needs of the land managers and the conditions of the area being interpreted.

The Interior Columbia Basin Ecosystem Management Project (ICBEMP) is an example of landscape analysis which used photo interpretation to produce a large robust dataset (Hessburg et al. 1999b, 1999c). As part of the ICBEMP analysis, over 300 watersheds were photo interpreted using early-19th-centry areal imagery (Hessburg et al. 1999a). This robust historical dataset has been commonly used as a reference target in forest restoration treatments, and is a major reason why the photo interpretation protocol as defined for ICBEMP has become so widely used regionally (Gaines et al. 2012). There are many different protocols that reflect the wide and varied use of photo interpretation (Spurr 1960; Avery 1969; Baker et al. 1997; Cosco 2011). However, no other methodology is associated with such a large and robust historical dataset as that of the ICBEMP dataset (Paul Hessburg, personal communications, June 4, 2018).

Areal Lidar is the measurement of terrestrial structure in three dimensional space using aircraft-mounted devices that measure the timing of returns from laser pulse emissions (Wulder et al. 2008). Lidar and Lidar products are increasingly being collected and produced for public forest lands (NOAA 2018; USGS 2018). Lidar data is able to capture structural information at fine scales and high levels of precision (Kaartinen et al. 2012). The formats of discrete return point cloud Lidar and its data products have opened new avenues of automated classifications of forest structural conditions (e.g. Wilkes et al. 2016; North et

al. 2017). Lidar and other fine scale remotely sensed data products are increasingly being used in forest management in place of photo interpretation products (Eid et al. 2004). Although these approaches have many advantages over photo interpretation, they also have many limitations. Lidar data are often very large and are not readily interpretable. Significant data reduction is necessary in order to produce data products that are useable for managers (Mcgaughey 2015). Often these data products are unintuitive to managers accustomed to working with remote sensing approaches that have longer established workflows (Jeronimo et al. 2017).

Large dataset and robust workflows exist for both the photo interpretation and Lidar methodologies. Both methodologies have unique and non-overlapping strengths in describing forest conditions. Bridging the data products of these methodologies would expand the capabilities for both approaches. The integration of Lidar data into the photo interpretation process could increase the pace of the interpretation process, as well as providing photo interpreters with additional information sources from which to make inferences. Finding relationships between data products could facilitate the creation of "photo interpretation-like products" derived from Lidar data, which would be accessible to land managers familiar with photo interpretation data formats. These relationships could also allow for the direct comparison of contemporary Lidar data to historical photo interpretation datasets. To my knowledge no previous studies have attempted to evaluate the comparability of photo interpretation datasets and Lidar data products.

The overarching goals of this study were to develop methods that incorporate Lidar products into the photo interpretation process, and to evaluate the comparability of Lidar products to photo interpretation attributes. My study objectives were to evaluate correlations between photo interpretation attributes and logical analog Lidar data products, develop models to predict photo interpretation attributes using Lidar data products as predictor variables, and summarize photo interpretation attributes and equivalent Lidar predicted attributes using watershed scale spatial pattern metrics to evaluate the substitutability of the datasets in a mid-scale analysis scenario. I built models to predict photo

interpretation attributes for individual photo interpretation patches, using metrics derived from Lidar data from within the patch boundaries. Model performance was assessed with regards to the level of agreement between the reported photo interpretation attributes and the corresponding predicted values.

2. Methods

2.1 Study Area

The 1.1-million-acre Colville National Forest (CNF) is located within the Okanagan highlands physiographic province of northeastern Washington (Figure 1). The CNF is divided into two major sections by the Columbia River. The western portion of the CNF, within which both study watersheds are located, is defined by the Kettle Crest: a mountain range running from north to south. The Kettle Crest possesses a cold semi-arid climate, characterized by cold wet winters, hot dry summers, and very wet transition seasons. The majority of the 25.8-inches (656 mm.) of precipitation that falls on the Kettle Crest occurs in the spring, with average monthly highs and lows of 3.0-inches (77 mm.) in June and 1.1-inches (29 mm.) in August. Fluctuations in temperature are moderate with monthly mean highs and lows of 76.8°F (24.9 °C) in August and 17.8°F (-7.9 °C) in December (PRISM Climate Group 2015).

The CNF exists in the Pseudotsuga menziesii Zone (Franklin and Dyrness 1973). The gradient of rainfall and elevation within the Kettle Crest creates a diverse range of forest communities. The western edges and low-elevation valleys of the CNF include warm, dry ponderosa pine (Pinus ponderosa) communities. Rainfall increases with elevation, with forest communities shifting to forests with increasing amounts of Douglas-fir (Pseudotsuga menziesii) and lodgepole pine (Pinus contorta). Above 3,000-feet elevation (914 m.), site conditions are increasingly cool and mesic, with western larch (Larix occidentalis), Engelmann spruce (Picea engelmanni), and subalpine fir (Abies lasiocarpa) becoming dominant. Western redcedar (Thuja plicata) occurs frequently in upland areas and near streams.

2.2 Data Collection

2.2.1 Photo Interpretation

The photo interpretation protocol that I employed in this study was adapted from the those described in the ICBEMP approach (Hessburg et al. 1999a). This approach is uniquely suited for the forested systems of the inland Pacific Northwest region, and it widely used by the USFS today (Michael Cibitski, personal communications, April 10 2018). The ICBEMP approach was developed as part of a large-scale effort to quantify the departure of contemporary watersheds from the range of conditions that were historically present in the region (Hessburg et al. 2000). This approach and the resulting historical dataset have been widely used in regional restoration efforts (Gaines et al. 2012). The protocol for individual watersheds includes an initial scouting of forest conditions to build a conceptual relationship between ground-observed and image-observed patterns. The watershed is then delineated into patches of four hectares or larger describing homogenous forest conditions. Patches are then attributed for a set of forest conditions. These first-order attributes are then processed though a set of dichotomous keys to classify forest structure and produce a set of indicator metrics classifying risk to various disturbances. Finally, the watershed is processed using FRAGSTATS to produce a set of landscape metrics for each attribute of interest. The range of values for a given metric across all historical watersheds of the same ecological sub-region represent the historical range of variability for a contemporary watershed (Keane et al. 2009).

The photo interpretation dataset I used in this study is comprised of two watersheds. The Orient watershed is a 9,458-hectare HUC 12 sub-watershed (ket0606). The watershed was photo interpreted by an experienced photo interpreter not associated with this project. A combination of high resolution (30 cm. by 30 cm.) stereo orthoimagery and Microsoft Bing imagery was used for this watershed. The data products for the Orient watershed were delivered to me by the CNF. Approximately 20% of Orient watershed extended outside the boundary of the Lidar data used in this study. Any photo interpretation patches that extended into this area were excluded from the study. The Bulldog watershed is a 17,824

hectare HUC 12 sub-watershed (ket0604). The watershed was not photo interpreted prior to this study. High resolution (30 cm. by 30 cm.) stereo orthoimagery was flown in late 2015 by the CNF and provided to me. Approximately 20% of the Bulldog watershed burned prior to the collection of the stereo orthoimagery, and after the collection of the Lidar data. Any photo interpretation patches that extended into the extent of the burn were excluded from this study. I carried out the methods described below on the Bulldog watershed only.

I collected field reference data in order to calibrate photo interpretation with ground-truth observations. Field reference points were randomly distributed across the watershed in an attempt to capture a wide range of extant variation in forest type, density, structure class, spatial pattern, management history, and disturbances. Point locations were chosen in the field, and were limited by road accessibility. At each point, I recorded a GPS location with a Garmin GLO consumer-grade GPS unit. I took one to three photos capturing site conditions of the immediate area, as well as diameter measurements in order to calibrate an estimate of size class for each canopy strata layer present. I recorded all photo interpretation metrics as observed on the ground for the immediate area. In total I collected 92 points within the Bulldog watershed boundary.

I preformed the delineation and attribution of the Bulldog watershed using DAT/EM Summit Evolution Version 7.4 (Summit) and ESRI ArcGIS ArcMap Version 10.5.1 (ArcMap) In tandem. The geospatial location of the cursor is synced between the two programs allowing for feature creation and manipulation in ArcMap, while viewing stereoscopic orthoimagery in Summit.

I delineated the Bulldog watershed first at a 1:12,000 scale before updating the delineation at a 1:8,000 scale. I identified patches as areas of contiguous forest equal to or greater than four-hectares in size, homogenous in pattern of all photo interpretation attributes. When a conditions within a single patch appeared to vary by a classification for any given metric, I split the patch into two distinct patches. I divided large patches at narrow points in order to minimize perimeter to area ratios. I aggregated and averaged interspersed patches less than four-hectares in size.

I attributed each delineated patch individually at a 1:1,800 scale. I calibrated my attribution calls by attempting to predict the conditions of each scouting point in the Bulldog area until I was able to predict scouting plot conditions within one attribute class consistently. For each delineated patch, I estimated average conditions across the entire patch area for each photo interpretation attribute. When specific attributes were uncertain, I identified one or more scouting plots closely matching the patches visual appearance and used the attributes of these plots to guide attribution of the patch. If delineations appeared to be inaccurate a the 1:1,800 scale, I would zoom the stereoscopic display to the 1:8,000 scale. If the delineation still appeared inaccurate, I would modify the delineation before continuing with the attribution.

Quality assurance was preformed both after the delineation and attribution phases by a secondary photo interpreter: James Begley of Washington Conservation Science. At both stages, five 400-hectare squares were randomly generated within the watershed boundary, describing approximately 20% of the study area. During the delineation quality assurance phase, the secondary photo interpreter delineated patches within these squares without prior knowledge of my delineation. We then compared our delineations together to identify inconsistencies. The secondary photo interpreter then made recommendations for improvements of the delineation overall. During the attribution quality assurance phase, my delineated patches were clipped to the box areas and stripped of their attributes. The secondary photo interpreter attributed these patches. Again we compared our attributions and I received recommendations for improvements.

Post processing done for the photo interpretation dataset included error checking and correcting and derivation of second order attributes. I ran error checking scripts to endure that all attributes were internally consistent for all patches (e.g. Overstory Canopy Cover was not greater than total Canopy Cover). Dichotomous keys produced by the PNW Research Station were run by the secondary photo interpreter in order to produce a set of second-order metrics describing ecological characteristics of each patch.

2.2.2 Lidar

Watershed Sciences, Inc. (Corvallis, OR), collected LiDAR data for a 171,091-acre area of the CNF between August 3rd and August 29th of 2014. Data were collected using a Leica ALS 60 sensor mounted to a Partenavia Aircraft. The acquisition was flown at 900-meters above ground level and captured a scan angle of ±15 degrees, resulting in an average pulse density of 9.9 pulses per square meter.

Final products delivered from Watershed Sciences included point cloud data of all returns and ground returns stored in LAS v.1.2 format, one-meter digital elevation models of bare earth ground models, and study area vector shapes. All data were projected in NAD83(2001), NaVD88 (Geoid 12A), United States Forest Service Region 6 Albers.

2.3 Analysis

The spatial grains of the photo interpretation and Lidar datasets are significantly different in scale. Photo interpretation data describes conditions at the resolution of the patch which is four-hectares or greater, while Lidar data reports spatial location at the resolution of 8 pulses per square meter. In order to create comparable datasets, I summarized Lidar data by photo interpretation patch area. For each patch of both watersheds in this study, I clipped the las points within the patch boundary. I normalized point heights to the one-meter Lidar digital terrain model. I processed the normalized point cloud datasets with FUSION CloudMetrics in order to produce a set of summary metrics describing the vertical point distribution for the patch area (Figure 2)(Mcgaughey 2015). I calculated canopy cover at height interval breaks of 2, 4, 8, 16, 32, and 48-meters. I defined canopy cover by strata as the proportion of returns that reached the depth of a strata layer and were intercepted at that layer.

I produced a canopy surface model with FUSION CanopyModel (Mcgaughey 2015). I identified tree approximate objects (TAOs) within the patch area with FUSION TreeSeg, which uses a watershed identification algorithm to identify canopy area occupied by one tree dominate to its immediate area and zero or more trees subordinate to the immediate area (Figure 3)(Jeronimo 2015; Mcgaughey 2015). I

ascribed the max height value of each TAO to the TAO area, and binned heights into ecologically meaningful height classes (Figure 4). The resulting layer effectively describes the canopy area of the patch segregated into height classes. I produced a set of FRAGSTATS metrics for each patch describing the proportion of patch area occupied by each height strata and number of patches in each height strata (McGarigal and Marks 1995). I also identified the number of large patches in each height strata, which I defined as 10 $m.^2$ or larger.

The photo interpretation metrics modeled in this study were the second-order metric, Structure Class, as well as the first-order metrics used in the dichotomous key that derives Structure Class (i.e. Number of Canopy Strata, Overstory Canopy Cover, Understory Canopy Cover, Overstory Size Class, and Understory Size Class). Structure Class is a commonly used and highly descriptive photo interpretation attribute. As Structure Class synthesizes many different aspects of forest structure, it is able to capture many of the forest conditions that are of interest to managers. Vertical forest structure is also an aspect of forest conditions which Lidar is known to explicitly describe (Kane et al. 2010b, 2014).

I modeled each photo interpretation attribute with RandomForest using Lidar derived metrics as training data (Table 1)(Breiman 2001). RandomForest is very useful in identifying variable importance by ranking the usefulness of predictor metrics in model predictive power. RandomForest is also able to overcome limitations of other modeling techniques because it relies on very few assumptions. Each photo interpretation patch was treated as a discrete observation. Modeling was done using a three-fold cross-validation model design. For each photo interpretation metric, the dataset was divided into three equal subsets. Each subset was stratified so that the frequency distribution of response variable class values matched that of the entire dataset. Three models were generated using two of the three subsets as training data and the remaining subset as testing data. This resulted in a wall-to-wall prediction of the study watersheds. A forth model was generated using the entire dataset in order to identify variable importance. I generated models using three subsets of the predictor variables. These subsets included the entire predictor dataset, an unsupervised subset of parsimonious predictors selected with the VSURF tool

(Genuer et al. 2015), and an a priori selection of predictors with easily interpretable relationships to the response variable. Structure Class was additionally derived from the dichotomous key using modeled first-order metrics.

I assessed model accuracy using confusion matrices. In the context of this study, model accuracy can be considered the level of agreement between the photo interpretation and Lidar datasets (the terms accuracy and agreement are used interchangeably in this thesis). Model accuracy was evaluated in terms of predicting the observed photo interpretation value. When evaluating ordinal attributes (i.e. Number of Canopy Strata, Overstory Canopy Cover, Understory Canopy Cover, Overstory Size Class, and Understory Size Class) model accuracy was additionally evaluated in terms of predicting within one class of the observed photo interpretation value. Attributes were binned into lower resolution classes, modeled, and predicted as well (Table 1).

I used the models with the highest levels of agreement with the photo interpretation dataset to create a prediction for the entire Bulldog dataset. I summarized the observed photo interpretation and predicted values of Structure Class using FRAGSTATS to produce a set of landscape metrics. I compared these metrics to the historical range of variation for the same ecological sub-region in the ICBEMP historical dataset.

3. Results

3.1 First-order metrics

Models describing Total Canopy Cover tended to have above average levels of precision (Table 2). The most common classes tended to have the lowest error rates (Figure 5). When binned into simplified bins, Total Canopy Cover matched observed photo interpretation values at higher rates, and had higher null accuracy values. Predictor metrics found to be most important in explaining variation for Total Canopy Cover include proportion of landscape covered by height strata 0 m. to 2 m., proportion of first returns above 2 m., and proportion of landscape covered in height strata 16 m. to 32 m.

Models describing Overstory Canopy Cover preformed at reduced levels of precision compared to Total Canopy Cover. Lower canopy cover values tended to have higher accuracy rates (Figure 6). Top predictor metrics for Overstory Canopy Cover include the percentage of first returns above the mean return height, as well as FRAGSTATS metrics describing the percentage of landscape at several height strata. There was very little fall-off in variable importance for predictor metrics. Models describing Understory Canopy Cover had similar accuracy rates to those of Overstory Canopy Cover. However, predictor metrics found to be most important in describing variation were mixed in terms of the logical relation to the response variable. Accuracy rates were highest in the class of zero canopy cover, and within one accuracy was highest in classes 0% to 20% (Figure 7). Top predictor variables include the proportions of land area covered by height strata 0 m. to 2 m. and 16 m. to 32 m., and KDE elevation minimum modal value.

Accuracy rates for models describing Overstory Size Class had nominal improvement over null predictions. Overstory Size Class values were dominated by small and medium values, which inflated the null accuracy (Figure 8). Top predictor metrics included elevation of returns in percentiles > 90 and proportion of land covered in upper canopy height strata. Accuracy rate for models describing Understory Size Class were similar to that of Overstory Size Class, but predictor variables found to be most descriptive had no apparent logical relations to the response variable. Accuracy rates were highest for the two most common size classes: no understory and poles (Figure 9).

When size class was simplified to a single value describing size class for the entire patch, predictive models performed better than those that predicted Overstory or Understory Size Class alone. Within one accuracy and null accuracy were both increased from individual canopy layer models (Figure 10). Top predictor metrics were similar to those observed for overstory size classes, and included proportion of land covered by upper canopy strata and in openings.

Predictive models describing Number of Canopy Layers preformed worse than the null hypothesis prediction. Attribute values were dominated by two canopy layers, with nominal proportions

of zero canopy layers and three or more canopy layers (Figure 11). Top predictor variables included elevations of returns in percentiles > 95, proportion of cover in lower height strata, and number of patches at various height strata.

3.2 Structure Class

Accuracy of models predicting Structure Class were moderate. Agreement rates were highest in the most common structure classes (Figure 12). When predictions were made with the dichotomous key using predicted first order metrics, predictions matched observed photo interpretation values much less frequently (Figure 13). Predictive models for Simplified Structure Class made predictions with higher accuracy and null accuracy (Figure 14). Top predictors for these models include proportion of land cover and number of patches at nearly all height strata.

3.3 Mid-scale analysis

A watershed scale comparison of observed photo interpretation Structure Class and predicted Structure Class showed similar patterns with regard to the historical dataset. Percent land cover of predicted Structure Class tended to be lower for all structure classes except for stand initiation, and understory reinitiation (Figure 15). All predicted classes were close in percent land cover to observed values except understory reinitiation. Patch density for structure classes was similarly low in departures (Figure 16). Predicted patch densities were lower than observed photo interpretation values except for stand initiation, which was higher.

4. Discussion

4.1 First-order metrics

Models predicting Total Canopy Cover agreed exactly with observed photo interpretation values at very low rates. However, these models predicted values within one value of the observed photo interpretation class with much higher accuracy rates. This pattern, combined with the higher accuracy

rates of the Simplified Canopy Cover metric, indicate that there is a relationship between what the photo interpreter is seeing, and what the Lidar data is capturing in terms of identifying the proportion of the patch in openings. However, it is likely that the resolution of 10% breaks may be too fine to consistently find exact agreement.

Generally, models that predicted attributes about individual canopy strata characteristics preformed worse than those models that summarized the characteristics for the entire patch. Models for both Canopy Cover and Size Class had higher accuracy rates when combined into a single value than when they were characterized as overstory and understory conditions. While this may be further evidence that agreement between photo interpretation and Lidar datasets is impractical at finer resolutions, it is also an indication of the limitations of this approach. Photo interpretation of overstory and understory canopy conditions is contextual in that the photo interpreter is making calls for the attributes considering only the portion of the patch that they selected as a distinct canopy layer. The Lidar metrics for this study summarized conditions across the entire patch. It is therefore unlikely that the Lidar data was able to accurately capture the conditions of individual canopy strata sufficiently.

Models that described individual canopy strata characteristics tended to have similar accuracy rates between overstory and understory conditions of the same attribute. However, models that predicted attributes about overstory characteristics often had much more logical predictor metrics. For Overstory Canopy Cover, top predictor metrics included the proportion of patch area in openings and in height strata 16 m to 32 m. This could be interpreted as the inverse of canopy cover and proportion of cover in the most common canopy class. Top predictor metrics for Understory Canopy Cover included patch area in openings and number of clumps in height strata 32 m. to 48 m. While the former metric is intuitive, there is little apparent connection between Understory Canopy Cover and the number of clumps in the tallest height strata. Similarly, the top predictors for Overstory Size Class was 99th percentile elevation and proportion of patch area in height strata 32 m. to 48 m. These metrics describe the tallest features of the patch which is intuitive. The top predictors for Understory cover percent were percent cover in height

strata 2 m to 4 m and number of openings. The relationship between these metrics and the attribute they are predicting is less clear.

The fundamental issue of the inability of the predictive models to agree with photo interpretation attributes of individual canopy layers is exemplified by the low agreement of the models predicting Number of Canopy Layers. A major challenge in modeling canopy layers was the low number of classes and the abundance of patches in the class of two canopy layers. The identification of individual canopy layers is something that has been attempted in previous studies with varying success (Wilkes et al. 2016). Without identification of individual canopy layers, it is unlikely that attributes describing overstory or understory canopy conditions could be predicted with acceptable accuracy levels.

Both the photo interpretation and airborne Lidar approaches are limited in that all data is collected above the canopy surface from an aircraft. While Lidar is capable of penetrating foliage, the fidelity of lower canopy layers is often low, especially in dense forest conditions (Kane et al. 2013). Likewise, areal imagery has a very clear view of the tallest features of a patch, but lower canopy conditions are often obscured by taller trees. Both data collection methods have much less information describing lower canopy conditions than overstory conditions. It is therefore intuitive that agreement between the two datasets would be lower when describing understory conditions. Photo interpretation metrics describing the understory are constrained in that they are dependent on corresponding overstory metrics to define allowable values. For example, Understory Size Class by definition cannot be larger than the Overstory Size Class; When only one canopy strata layer is present the Understory Canopy Cover will be equal to zero. That lower canopy cover values and smaller size classes tended to have higher levels of precision for understory metrics may be evidence that these models relied on coincidental patterns in predicting these most common lower classes. It is likely that these models describing understory conditions are overfitting to a large degree.

Simplified metrics had higher levels of precision than models predicting the original classes. Accuracy rates of predictions within one class of the observed value were much higher than exact

matching for all models. There is a clear indication that relationships exist between the Lidar and photo interpretation datasets. However, it is evident that the corresponding patterns between the two datasets may exist at a coarser resolution than those which are reported in the photo interpretation attribute classes.

4.2 Structure Class

Structure Class attributes were predicted with moderate success, yet it is difficult to determine if the predictor metrics used for these models have any ecological relationship to the response variable. Structure Class as defined by the photo interpretation protocol relies on multiple aspects of patch conditions in interacting ways. The nuanced nature of these class definitions precludes a simple interpretation of the predictor variables. Unlike understory metrics, there is no simple expectation for the relationship between the predictor and response variables.

4.3 Mid-scale analysis

The agreement between observed photo interpretation values and predicted values was low across nearly all models. However, watershed scale analysis of Structure Class using predicted values showed minimal departure from the observed conditions. This approach is essentially the use case for this methodology and historical dataset. This watershed scale approach to photo interpretation modeling appears to have potential. A much larger sample size would be necessary to explore the value of a watershed scale approach.

5. Conclusion

In interpreting the results of this study, it is important to do so within the scope of the original objectives. This study was not intended or designed to be an evaluation of the quality or accuracy of either dataset. Without a true ground-truth dataset, it is impossible to evaluate how well either method was able to summarize the conditions of the two watersheds of this study. An accuracy assessment of either methodology would be challenging, and a direct comparison of the accuracy of each methodology would carry significant complications and ambiguities. The difference in resolutions of the two datasets

preclude a direct three-way comparison. The goal of this study was to evaluate the comparability of these two remote sensing approaches. It is obvious that both methodologies are useful in describing forest conditions. Therefore, when models in this study fail to accurately predict photo interpretation metrics, the inference that should be drawn is that there is a lack of apparent agreement between the two approaches in describing a specific forest condition.

A major challenge in comparing these two methodologies is overcoming the fundamental misalignment in resolution of the approaches. The photo interpretation process relies on segmentation of forest pattern across the watershed. The photo interpreter is forced to work with constraints during the delineation process including a lower patch size limit and a reduction of patch area to perimeter ratio. These limitations can result in the creation of divisions across a gradient of conditions, and the inclusion of anomalous minority conditions in patches. During the attribution process, the photo interpreter attempts to summarize the resulting variation on forest structural conditions. This approach has the potential to produce metrics which describe the average or majority condition of the patch, and is often taken in the context of the contrast between the patch of interest and its adjacent patches (Figure 17).

Lidar data is reported at the resolution of a single pulse, and is summarized as the distribution of pulses in space for a given area. In order to compare these two datasets, the finer grained Lidar must then be reduced to the grain of the photo interpretation dataset. In attempting a direct comparison between these two datasets, I was forced to presuppose the delineated patches. By summarizing the Lidar data, equal weight is given to all returns within the patch area, which is fundamentally different than the "majority approach" that a photo interpreter would take. While a photo interpreter might discount anomalous minority conditions, this is not so for the approach I took with the Lidar data.

The photo interpretation process is highly iterative and contextual. A photo interpreter relies on a sequence of attribution to provide scope for subsequent attributions. In making decisions during the attribution process, the photo interpreter often only considers a subset of the total patch area. For example, the identification of unique canopy layers provides the context for which portions of the patch

area should be considered for strata specific attributes. A major limitation of this study was an inability to identify unique canopy layers. All models generated in this study considered all portions of the patch area in modeling each attribute.

While it is beyond the scope of this study to question the accuracy of these delineations in partitioning variation in forest structure, it is worth exploring the extent to which this approach addresses the ecological questions driving landscape analysis. The concept of the stand as a unit of forest area is pervasive and enduring (Franklin et al. 2018). Forest management has historically relied on the concept of the stand to operationalize forest management and inventory (Puettmann et al. 2010). The recent shifts in expanding the extent of forest inventory from the stand scale to the landscape scale has brought with it a shift from the stand level grain to a finer, tree neighborhood grain (Hessburg et al. 2015). We are increasingly moving form a stand based view of forests to a multiscale perspective (Turner 2010). This shift has been facilitated both by advances in our understanding of landscape ecology and by the advances in our remote sensing methods.

Characterizations of forest conditions are useful insofar as they are able to answer the questions that people have about the forests. Both photo interpretation and Lidar have clear utility in that they are widely used today. Both have unique strengths, and although they are often attempting to answer similar questions about forest conditions, they do so with different sets of assumptions. This study illustrates how there is a need to reconcile the assumptions in order to integrate these remote sensing approaches. However, a more important need may be to challenge the necessity of the assumptions themselves.

6. Acknowledgements

I thank Jerry Franklin, Van Kane, Derek Churchill and Monika Moskal for serving on my committee. Each was and continues to be a unique source of inspiration and support in their own way, without which I would likely not have completed or even started my master's program. I thank Sean Jeronimo and Russell Kramer for their support as peers during the master's process. The friendship and sense of community I found in these people was invaluable. I thank Paul Hessburg and Nick Povak for providing data and consultation on the historical dataset. I thank James Begley and Michael Chibicki for training me to use the photo interpretation process. I thank my partner and peer, Caileigh Shoot, for her love and encouragement. Finally, I thank Bridget Daly and John LeFevre for their continued love and support. Were it not for them I never would have challenged myself to achieve this.

7. Citations

Avery, T. E. 1969. *Interpretation of Aerial Photographs*. Second. Burgess Publishing Company, Minneapolis. 324 p.

Baker, B. W., R. D. Baker, S. Baker, M. Barber, and T. Beaumont. 1997. *Manual of Photographic Interpretation*. Second. Philipson, W.R. (ed.) American Society of Photogrammetry and Remote Sensing, Bethesda, Maryland. 698 p.

Breiman, L. 2001. Random forests. *Mach. Learn.* 45(1):5–32.

Churchill, D. J., A. J. Larson, M. C. Dahlgreen, J. F. Franklin, P. F. Hessburg, and J. A. Lutz. 2013. Restoring forest resilience: From reference spatial patterns to silvicultural prescriptions and monitoring. *For. Ecol. Manage.* 291:442–457.

Cosco, J. 2011. *Common Attribute Schema (CAS) for Forest Inventories Across Canada*. 117 p.

Eid, T., T. Gobakken, and E. Næsset. 2004. Comparing stand inventories for large areas based on photo-interpretation and laser scanning by means of cost-plus-loss analyses. *Scand. J. For. Res.* 19(6):512–523.

Franklin, J. F., and C. T. Dyrness. 1973. *Natural vegetation of Oregon and Washington*. Oregon State University Press. 417 p.

Franklin, J. F., K. N. Johnson, and D. L. Johnson. 2018. *Ecological Forest Management*. First. Waveland Press, Inc., Long Grove.

Gaines, W. L., D. W. Peterson, C. A. Thomas, and R. J. Harrod. 2012. *Adaptations to Climate Change : National Forests*. 34 p.

Genuer, R., J. Poggi, and C. Tuleau-malot. 2015. VSURF : An R Package for Variable Selection Using Random Forests. *R J.* 7(December):19–33.

Hessburg, P. F., D. J. Churchill, A. J. Larson, R. D. Haugo, C. Miller, T. A. Spies, M. P. North, et al. 2015. Restoring fire-prone Inland Pacific landscapes: seven core principles. *Landsc. Ecol.* 30(10):1805–1835.

Hessburg, P. F., R. B. Salter, M. B. Richmond, and B. G. Smith. 2000. Ecological subregions of the interior Columbia Basin, USA. *Appl. Veg. Sci.* 3:163–180.

Hessburg, P. F., R. B. Salter, B. G. Smith, S. D. Kreiter, C. A. Miller, C. H. McNicoll, and W. J. Hann. 1999a. Historical and current forest and range landscapes in the interior Columbia River basin and portions of the Klamath and Great Basins. Part I: Linking vegetation patterns and landscape vulnerability to potential insect and pathogen disturbances. *Gen. Tech. Reports US Dep. Agric. For. Serv.* (PNW-GTR-458):1–357.

Hessburg, P. F., B. G. Smith, C. Miller, S. D. Kreiter, and R. B. Salter. 1999b. Modeling change in potential landscape vulnerability to forest insect and pathogen disturbances: Methods for forested subwatersheds sampled in the midscale interior Columbia River basin assessment. *Gen. Tech. Reports US Dep. Agric. For. Serv.* (PNW-GTR-454):1–56.

Hessburg, P. F., B. G. Smith, and R. B. Salter. 1999c. Using estimates of natural variation to detect ecologically important change in forest spatial patterns: A case study, Cascade Range, eastern Washington. *USDA For. Serv. - Res. Pap. RMRS.* (PNW-RP-514):1–65.

Jeronimo, S. M. A. 2015. LiDAR individual tree detection for assessing structurally diverse forest

landscapes. *Univ. Washingt.* :65.

Jeronimo, S. M. A., L. R. Dow, V. R. Kane, D. J. Churchill, and J. F. Franklin. 2017. *Using LiDAR to Inform Silvicultural Restoration in the Crater Lake Panhandle Final Report to National Park Service PNW Cooperative Agreement H8W07110001*.

Kaartinen, H., J. Hyyppä, X. Yu, M. Vastaranta, H. Hyyppä, A. Kukko, M. Holopainen, et al. 2012. An international comparison of individual tree detection and extraction using airborne laser scanning. *Remote Sens.* 4(4):950–974.

Kane, V. R., J. D. Bakker, R. J. McGaughey, J. A. Lutz, R. F. Gersonde, and J. F. Franklin. 2010a. Examining conifer canopy structural complexity across forest ages and elevations with LiDAR data. *Can. J. For. Res.* 40:774–787.

Kane, V. R., J. A. Lutz, S. L. Roberts, D. F. Smith, R. J. McGaughey, N. A. Povak, and M. L. Brooks. 2013. Landscape-scale effects of fire severity on mixed-conifer and red fir forest structure in Yosemite National Park. *For. Ecol. Manage.* 287:17–31.

Kane, V. R., R. J. McGaughey, J. D. Bakker, R. F. Gersonde, J. A. Lutz, and J. F. Franklin. 2010b. Comparisons between field- and LiDAR-based measures of stand structural complexity. *Can. J. For. Res.* 40(4):761–773.

Kane, V. R., M. P. North, J. A. Lutz, D. J. Churchill, S. L. Roberts, D. F. Smith, R. J. McGaughey, J. T. Kane, and M. L. Brooks. 2014. Assessing fire effects on forest spatial structure using a fusion of Landsat and airborne LiDAR data in Yosemite National Park. *Remote Sens. Environ.* 151:89–101.

Keane, R. E., P. F. Hessburg, P. B. Landres, and F. J. Swanson. 2009. The use of historical range and variability (HRV) in landscape management. *For. Ecol. Manage.* 258(7):1025–1037.

Lertzman, K. P., and J. Fall. 1998. From forest stands to landscapes: spatial scales and the roles of disturbances. P. 339–367in*Ecological scale: theory and applications*,Peterson, D.L., and V.T. Parker (eds.).Columbia University Press, New York.

McGarigal, K., and B. J. Marks. 1995. FRAGSTATS: Spatial Pattern Analysis Program for Quantifying Landscape Structure. *Gen. Tech. Rep. PNW-GTR-351. USDA.* (August):1–122.

Mcgaughey, R. J. 2015. *FUSION/LDV: Software for LIDAR Data Analysis and Visualization*. 182 p.

NOAA. 2018. Data Access Viewer. Available online at: https://coast.noaa.gov/dataviewer/#/; last accessed June 18, 2018.

North, M. P., J. T. Kane, V. R. Kane, G. P. Asner, W. Berigan, D. J. Churchill, S. Conway, et al. 2017. Cover of tall trees best predicts California spotted owl habitat. *For. Ecol. Manage.* 405(July):166–178.

Noss, R. F. 2001. Society for Conservation Biology Beyond Kyoto: Forest Management in a Time of Rapid Climate Change. *Conserv. Biol.* 15(3):578–590.

PRISM Climate Group. 2015. Average monthly and annual climate conditions over the most recent three full decades. *Oregon State Univ.* Available online at: http://prism.oregonstate.edu.

Puettmann, B. K. J., K. D. Coates, C. Messier, I. Press, and K. Puettmann. 2010. A Critique of Silviculture : Managing for Complexity. *For. Sci.* 56(2):231–232.

Spurr, S. H. 1960. *Photogrammetry and Photo-Interpretation*. Second. The Ronald Press Company, New York. 472 p.

Turner, M. G. 2010. Disturbance and landscape dynamics in a changing world. *Ecology*. 91(10):2833–2849.

USGS. 2018. The National Map. Available online at: https://nationalmap.gov/3DEP/3dep_prodserv.html; last accessed June 18, 2018.

Wilkes, P., S. D. Jones, L. Suarez, A. Haywood, A. Mellor, W. Woodgate, M. Soto-Berelov, and A. K. Skidmore. 2016. Using discrete-return airborne laser scanning to quantify number of canopy strata across diverse forest types. *Methods Ecol. Evol.* 7(6):700–712.

Wulder, M., J. C. White, M. A. Wulder, C. W. Bater, N. C. Coops, T. Hilker, and J. C. White. 2008. The role of LiDAR in sustainable forest management The role of LiDAR in sustainable forest management. 84(September 2016).

8. Figures

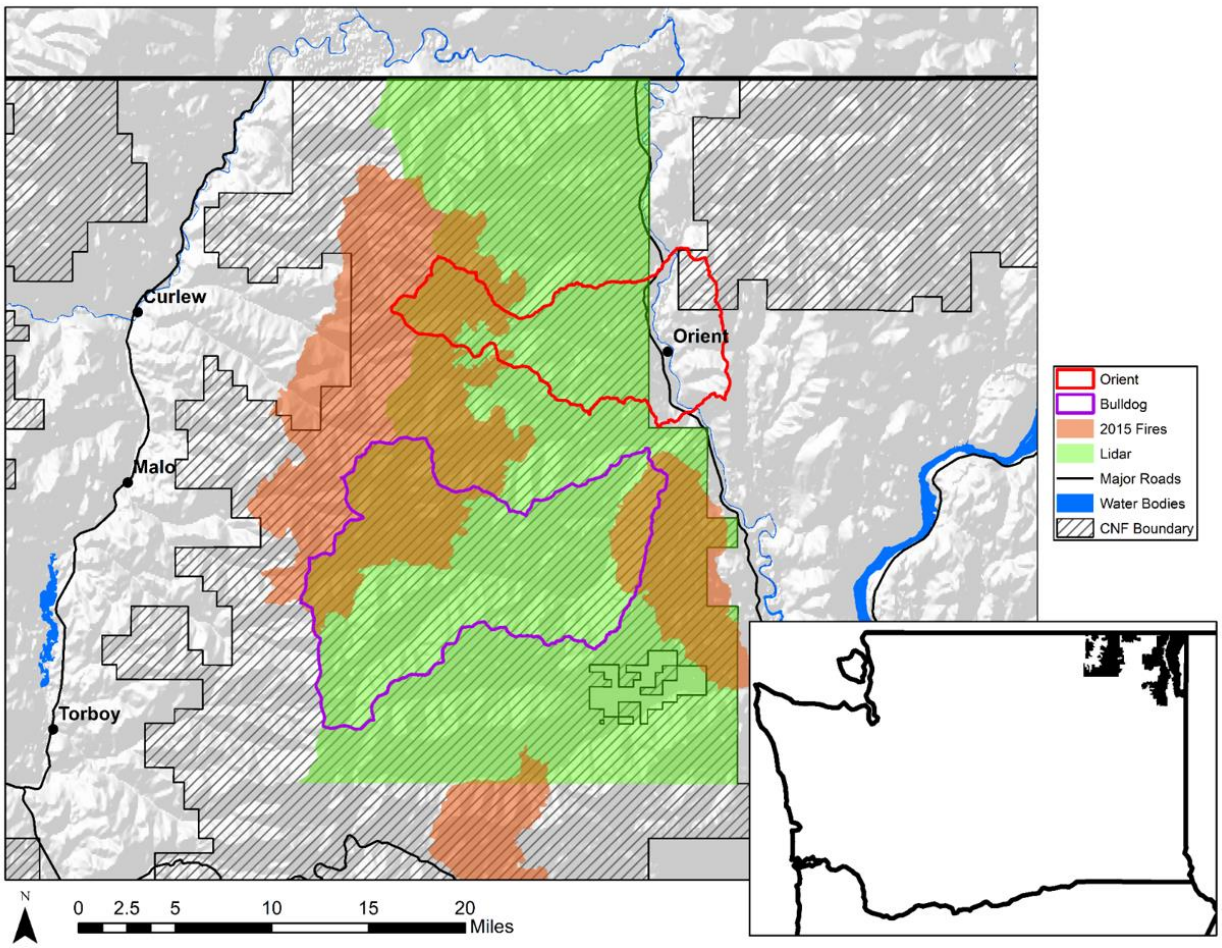

Figure 1. Study area map located in the Colville National Forest (inset). The two watersheds used in this study are the Orient watershed (red outline), and the Bulldog watershed (purple outline). The Orient watershed only partially overlapped the Lidar dataset (green area). The photo interpretation of the Bulldog watershed was limited to the areas that did not burn in the 2015 fires (orange area).

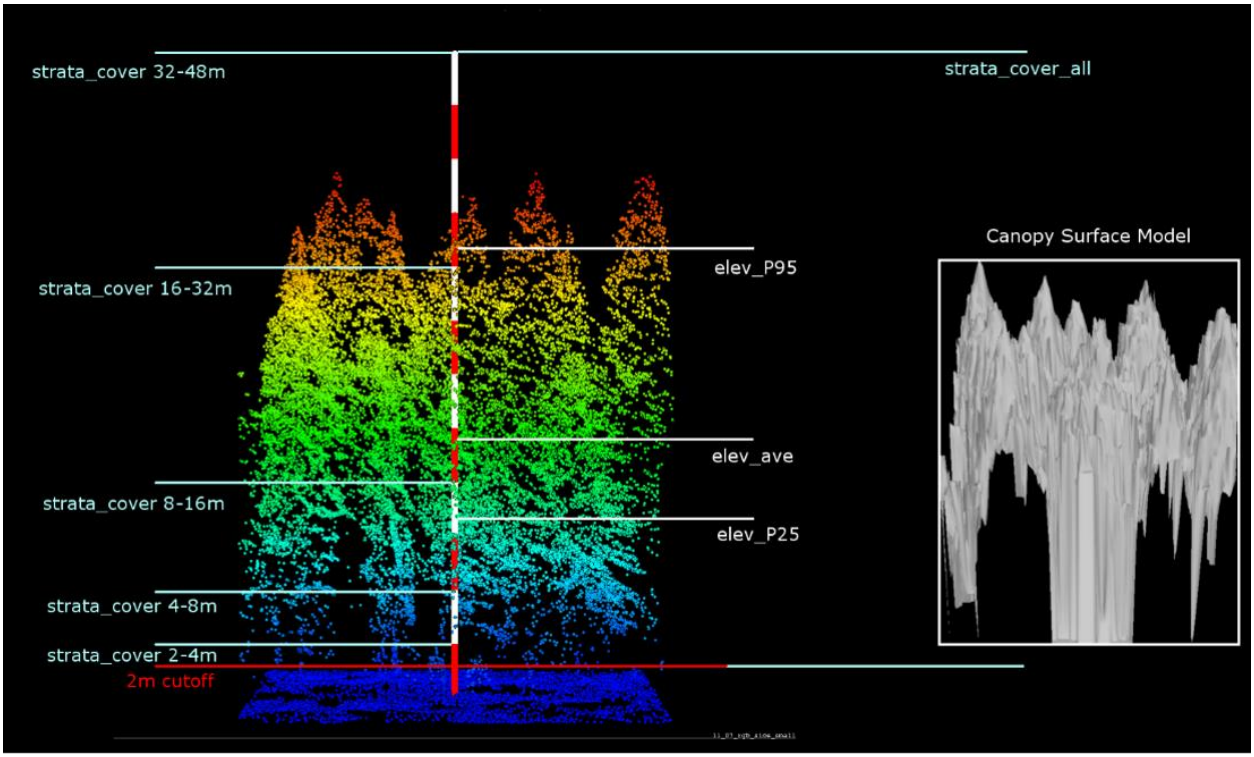

Figure 2. Illustration of key vertical structure metrics calculated with FUSION CloudMetrics. Strata cover metrics on the left of the height pole are calculated as the proportion of returns that reached the strata (represented as the area between the horizontal white lines) and were intercepted. Elevation metrics are the height values of statistical reductions (e.g. percentile or averages) of the point cloud. A canopy surface model (right) was also generated.

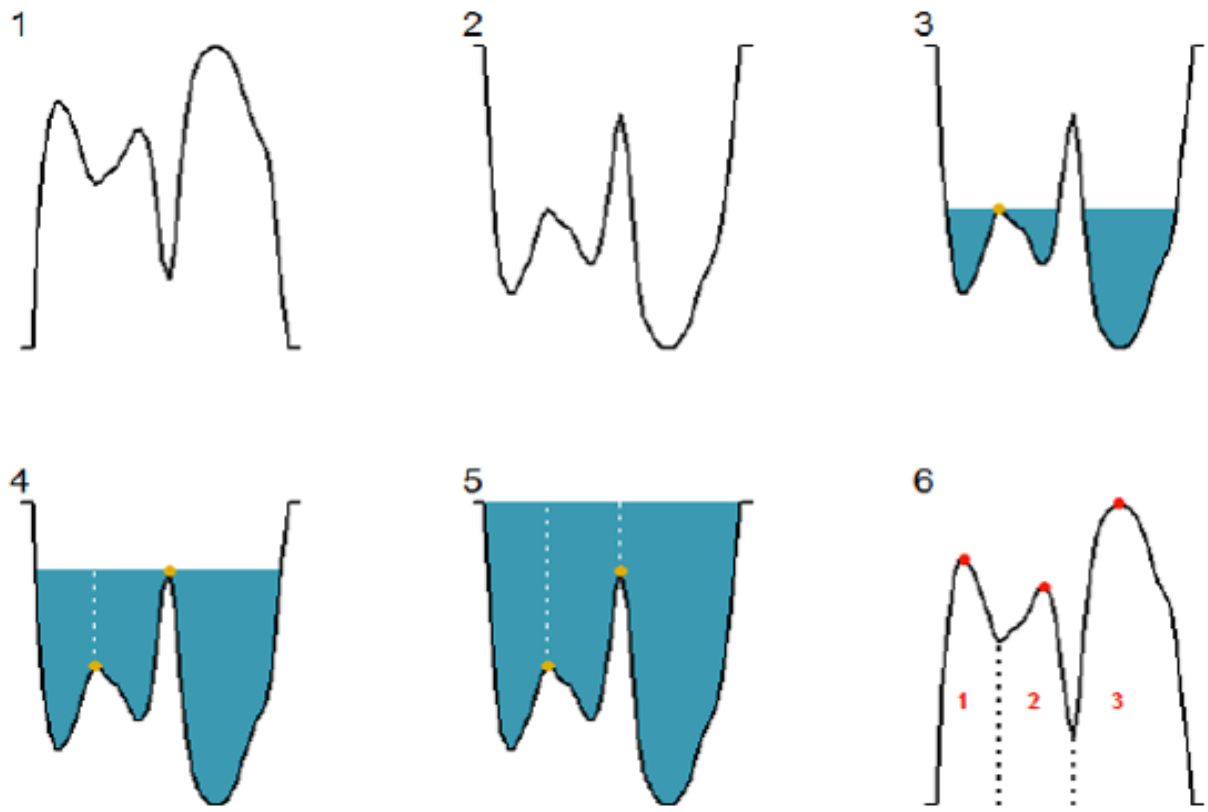

Figure 3. Overview of the watershed segmentation algorithm, presented here as a 2D concept, but actually performed in 3D. (1) The canopy surface model is draped over the LiDAR point cloud. (2) The canopy surface model is inverted (3-5). The surface is imagined to be made of a permeable material, and is slowly lowered into water. Any time two separate pools come into contact (yellow points), a dam (white dashed lines) is formed. (6) The canopy surface model is righted. The dams are taken to be region boundaries, and high points within each region so defined are taken to be the treetops (red points).

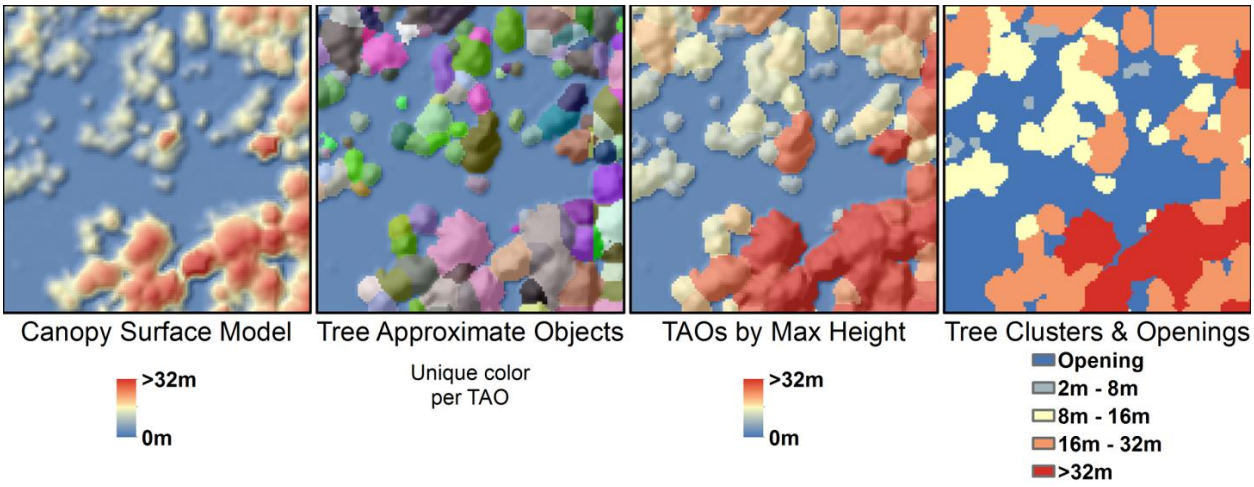

Figure 4. Identification and measurement of tree clusters, tree clumps, and openings from LiDAR-derived canopy surface models was done in four steps: (1) create a 0.75 m resolution canopy surface model, (2) identify immediately dominant tree approximate objects (TAOs) using a watershed segmentation, (3) assign the area of each TAO the maximum height of that TAO, (4) classify each TAO by height strata (2 to 8, 8 to 16, 16 to 32, and >32 m; openings are <2 m). Tree clusters are one or more adjacent TAOs in the same height strata while tree clumps are one or more adjacent tree clusters separated from other tree clumps by openings.

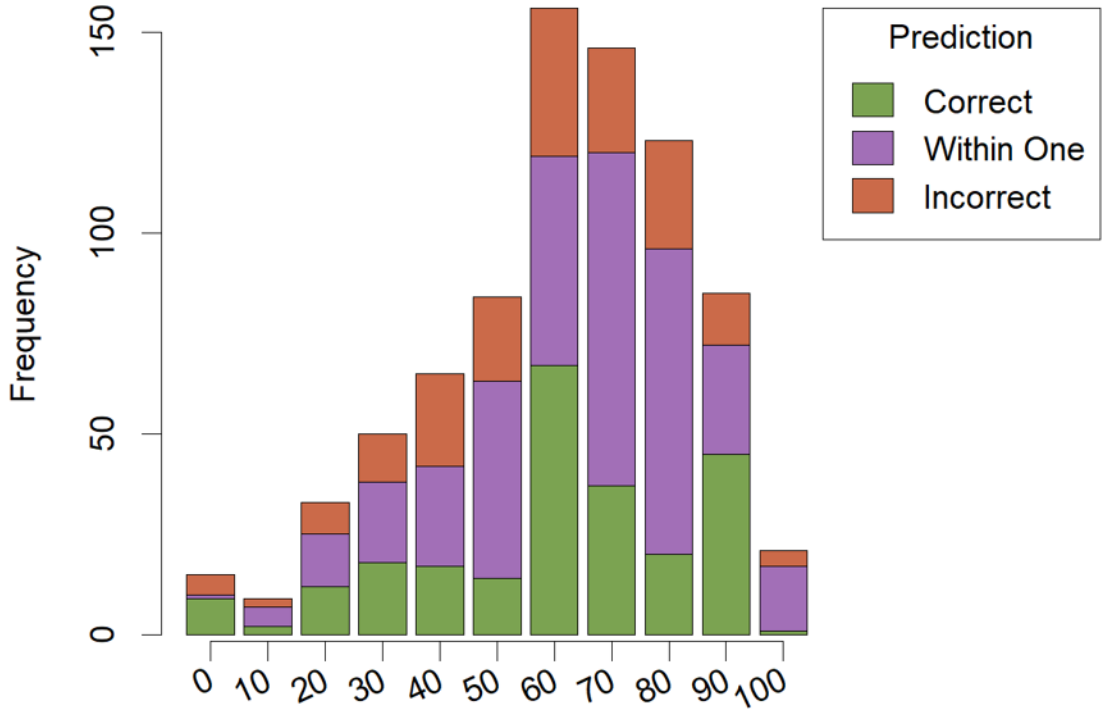

Figure 5. Histogram of observed photo interpretation values of Total Canopy Cover by patch. Colors correspond to model agreement in predicting photo interpretation values.

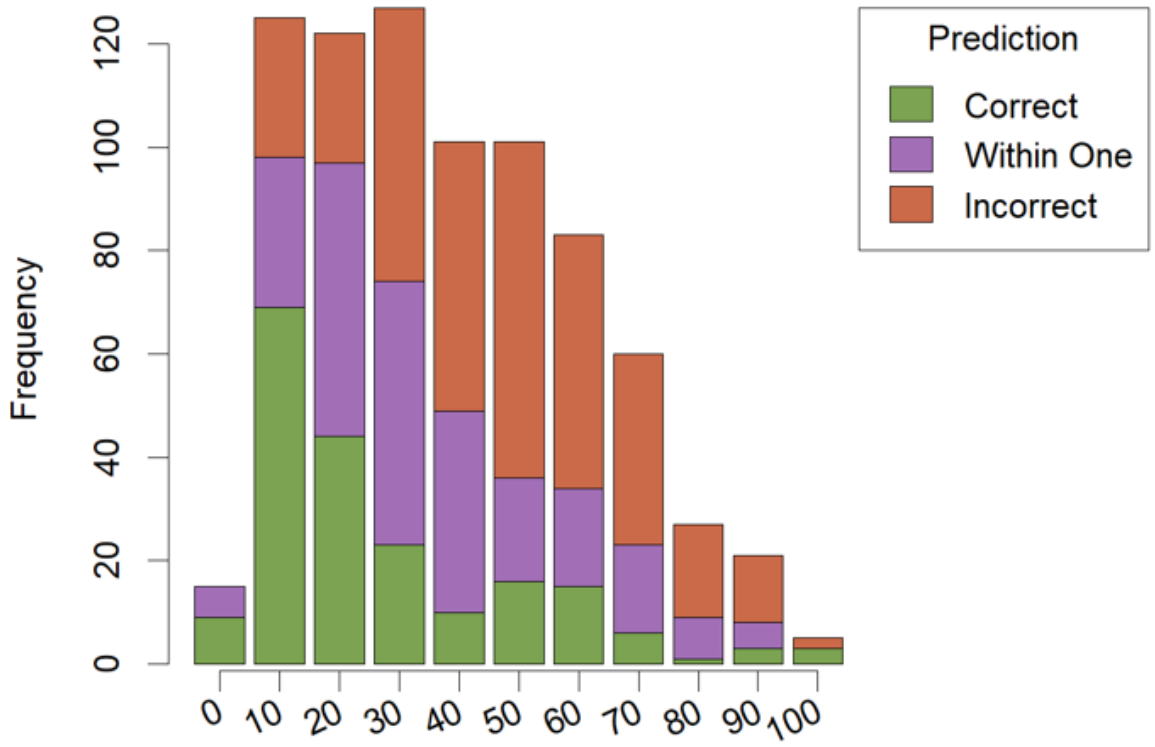

Figure 6. Histogram of observed photo interpretation values of Overstory Canopy Cover by patch. Colors correspond to model agreement in predicting photo interpretation values.

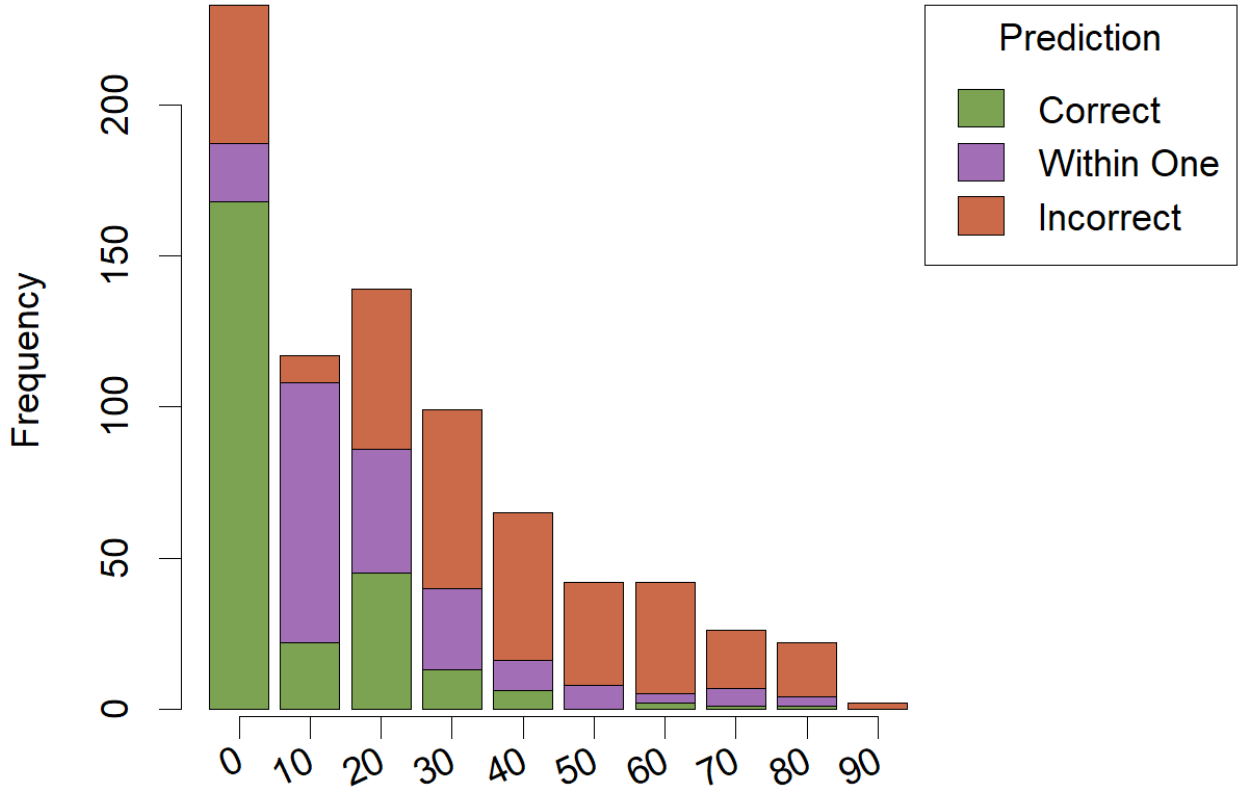

Figure 7. Histogram of observed photo interpretation values of Understory Canopy Cover by patch. Colors correspond to model agreement in predicting photo interpretation values.

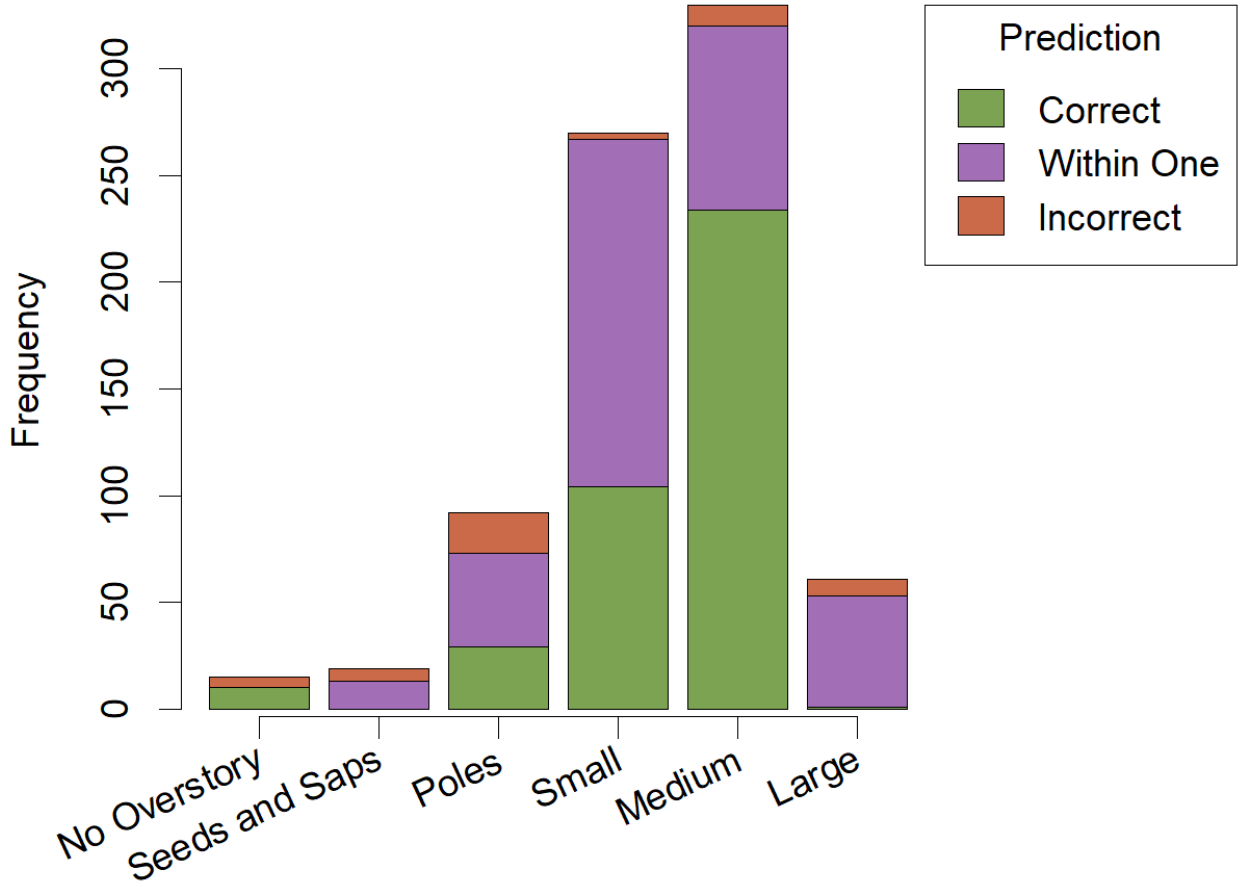

Figure 8. Histogram of observed photo interpretation values of Overstory Size Class by patch. Colors correspond to model agreement in predicting photo interpretation values.

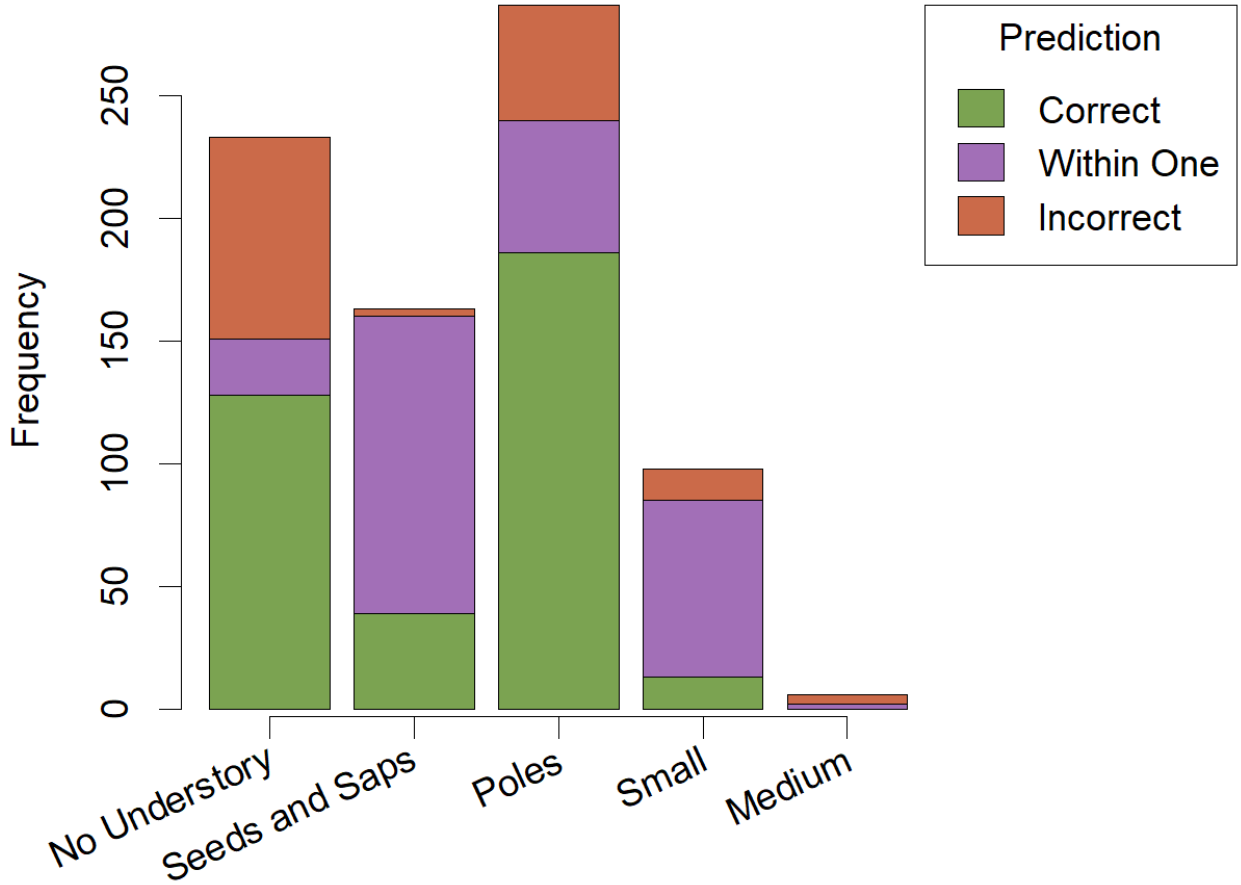

Figure 9. Histogram of observed photo interpretation values of Understory Size Class by patch. Colors correspond to model agreement in predicting photo interpretation values.

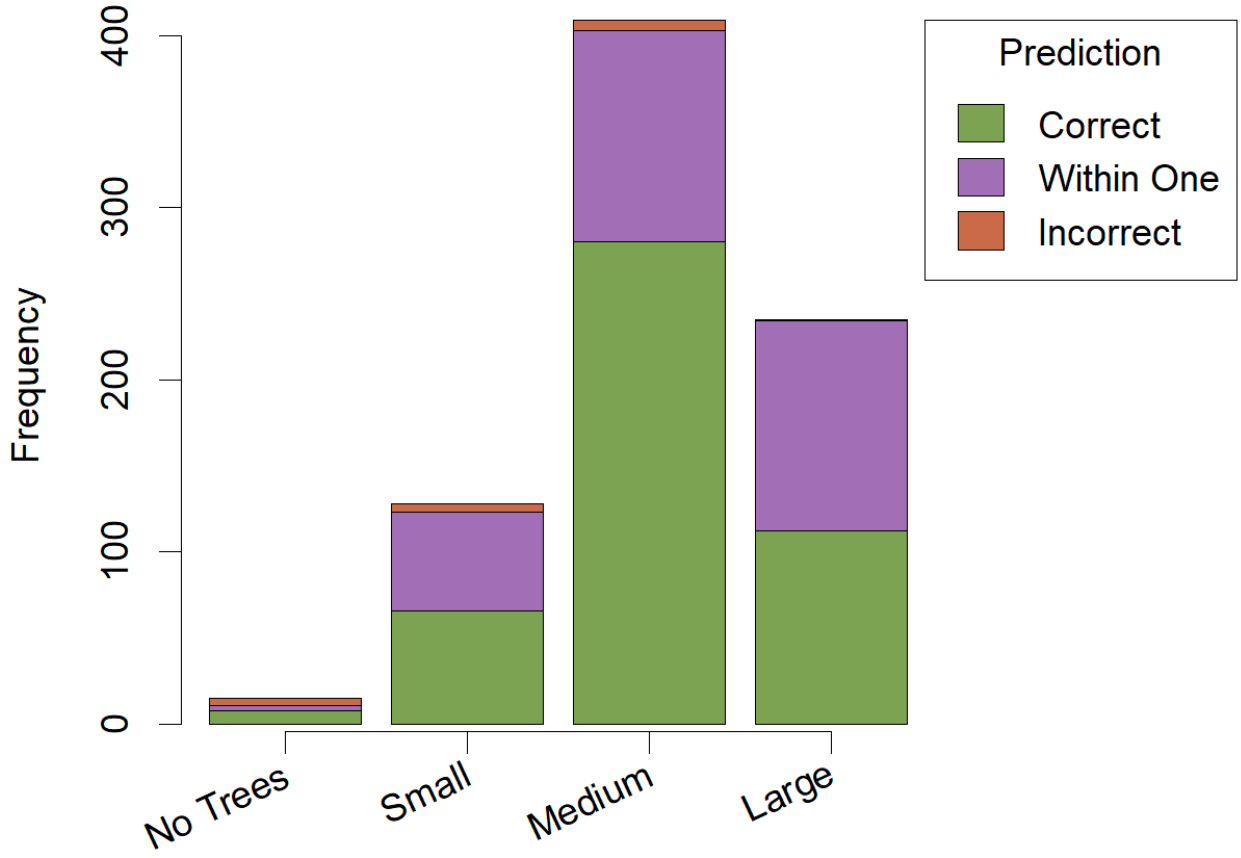

Figure 10. Histogram of observed photo interpretation values of Simplified Size Class by patch. Colors correspond to model agreement in predicting photo interpretation values.

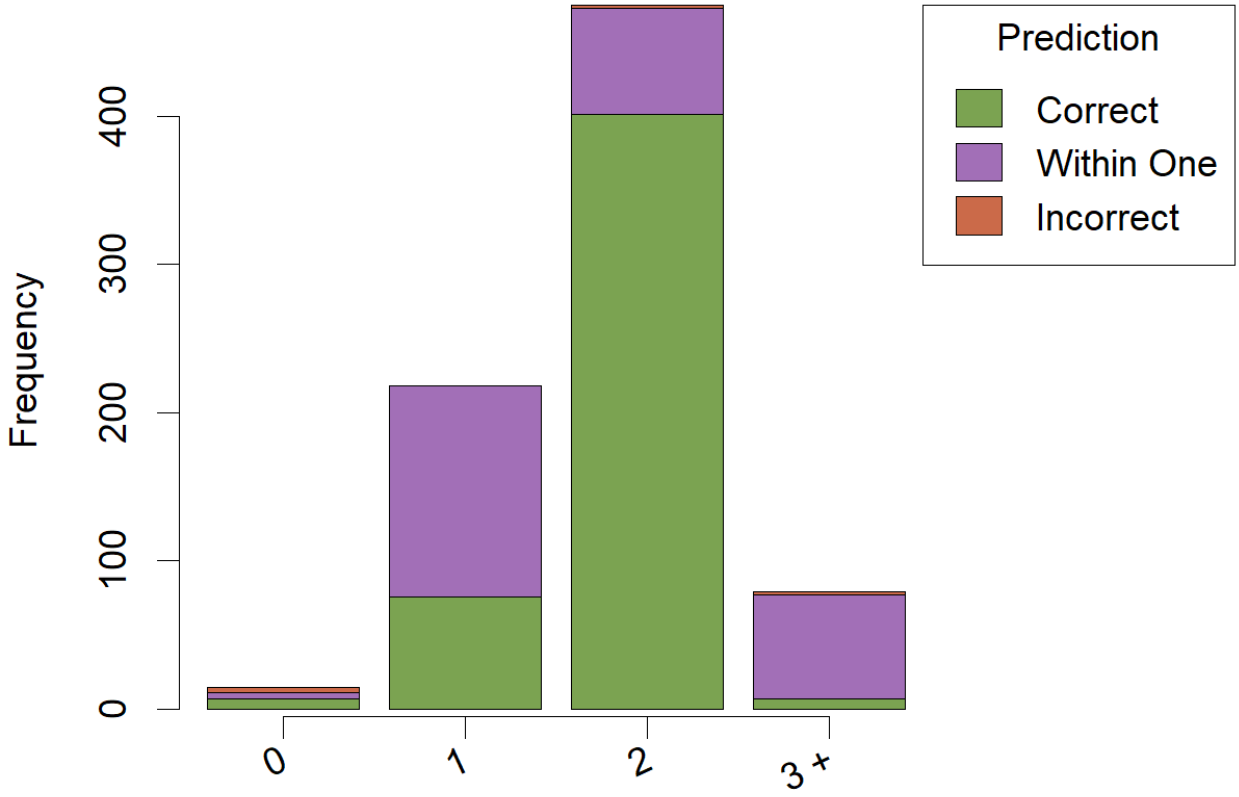

Figure 11. Histogram of observed photo interpretation values of Number of Canopy Layers by patch. Colors correspond to model agreement in predicting photo interpretation values.

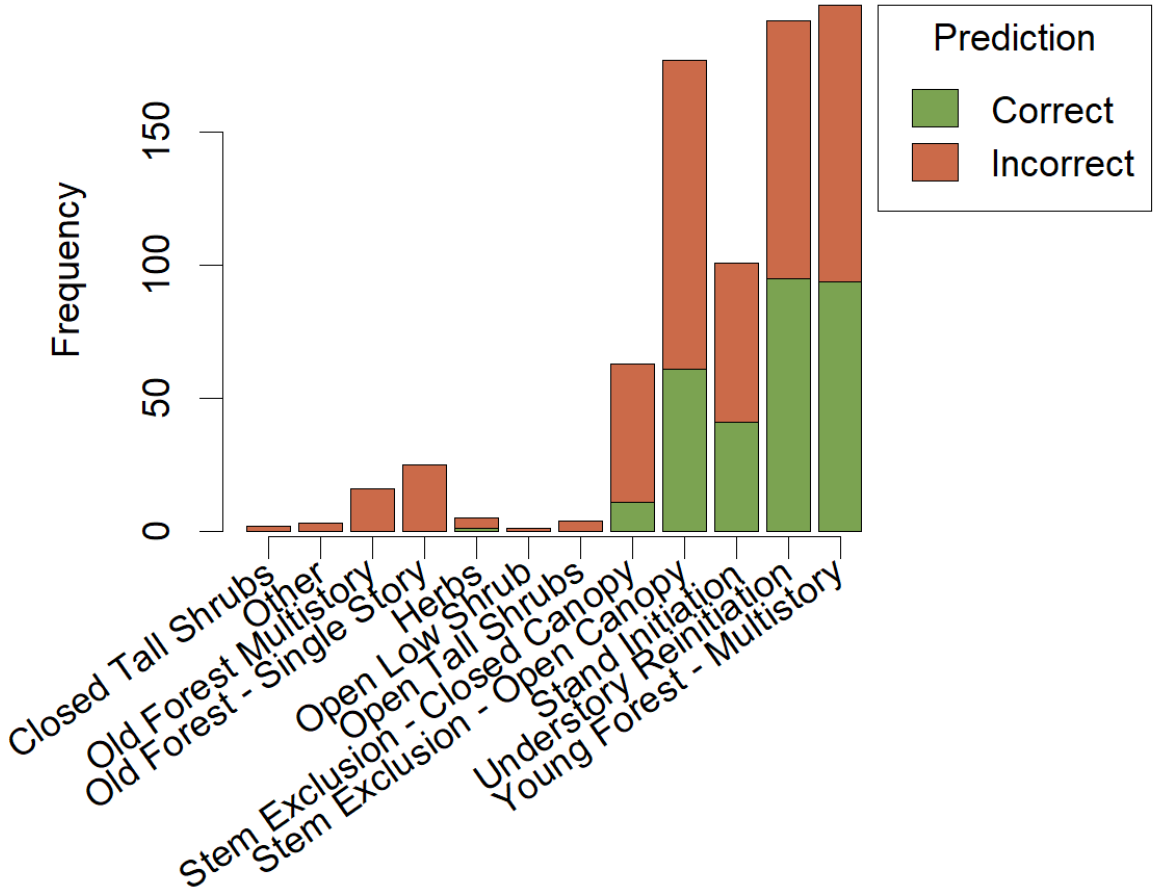

Figure 12. Histogram of observed photo interpretation values of Structure Class by patch. Colors correspond to model agreement in predicting photo interpretation values using a Lidar trained RandomForest model.

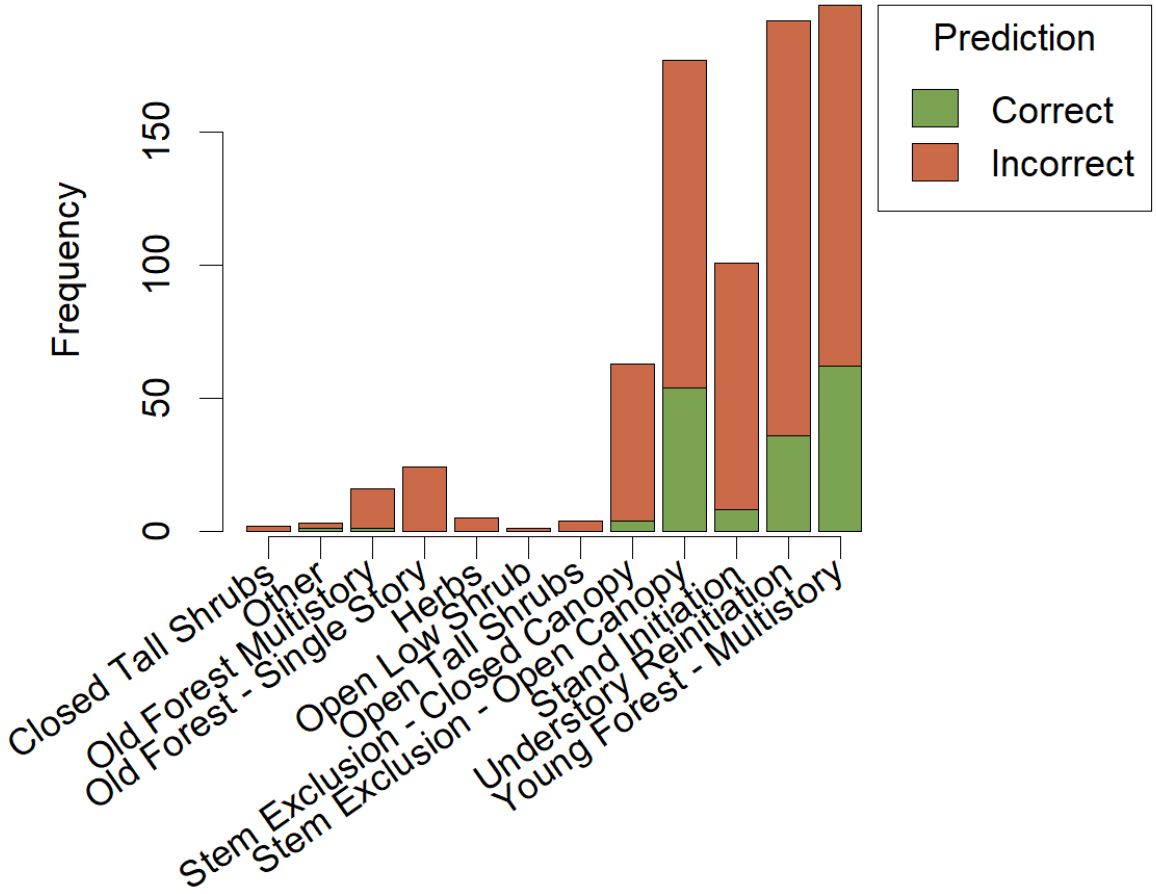

Figure 13. Histogram of observed photo interpretation values of Structure Class by patch. Colors correspond to model agreement in predicting photo interpretation values from dichotomous key classifications using predicted first-order attributes.

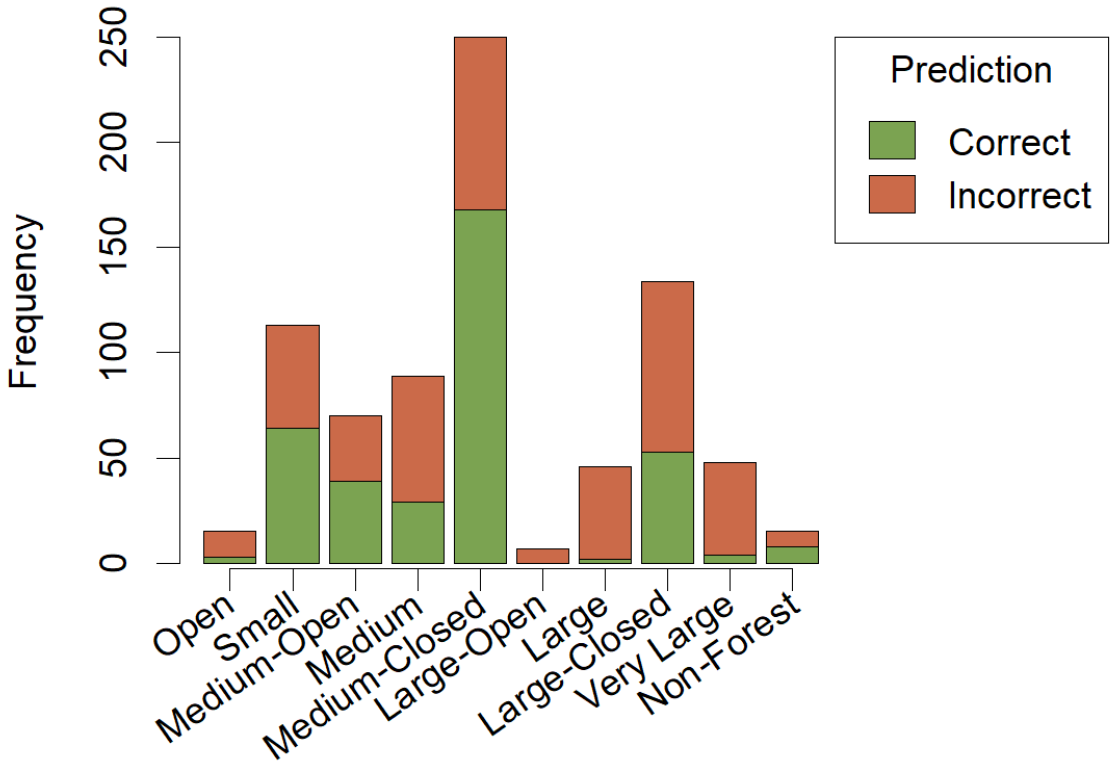

Figure 14. Histogram of observed photo interpretation values of Simplified Structure Class by patch. Colors correspond to model agreement in predicting photo interpretation values.

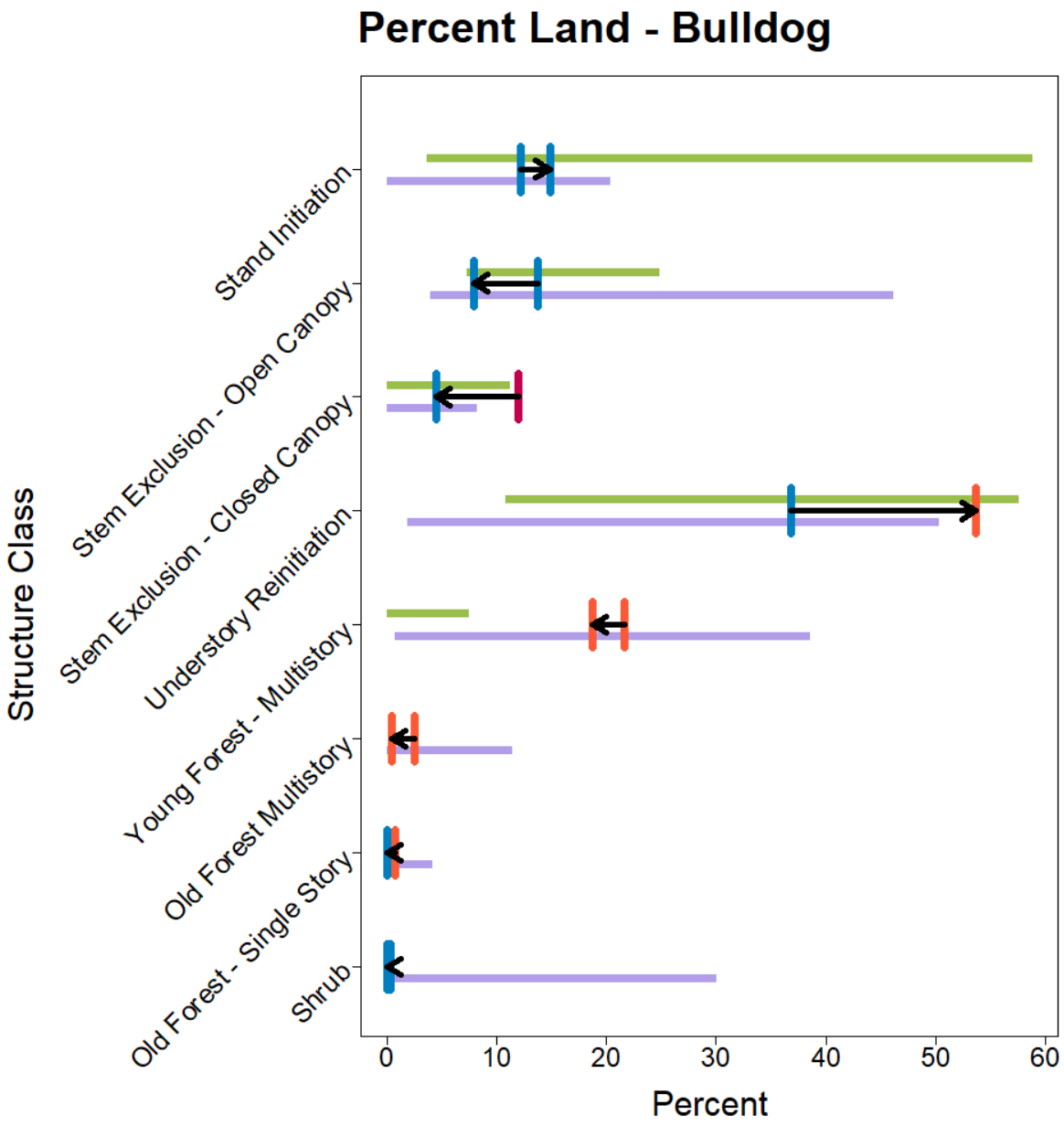

Figure 15. Midscale analysis of percent land cover for the Bulldog watershed using observed and predicted photo interpretation Structure Class. Green bars represent the range of conditions in the HRV dataset for the same ecological sub-region (ESR). Purple bars represent the range of conditions for the next warmest/driest ESR. Vertical bars represent the observed and predicted watershed scale values, with the arrow showing the direction of departure from the observed value. This figure shows how a land manager might identify aspects of watershed conditions departed from reference conditions and in need of restoration treatments.

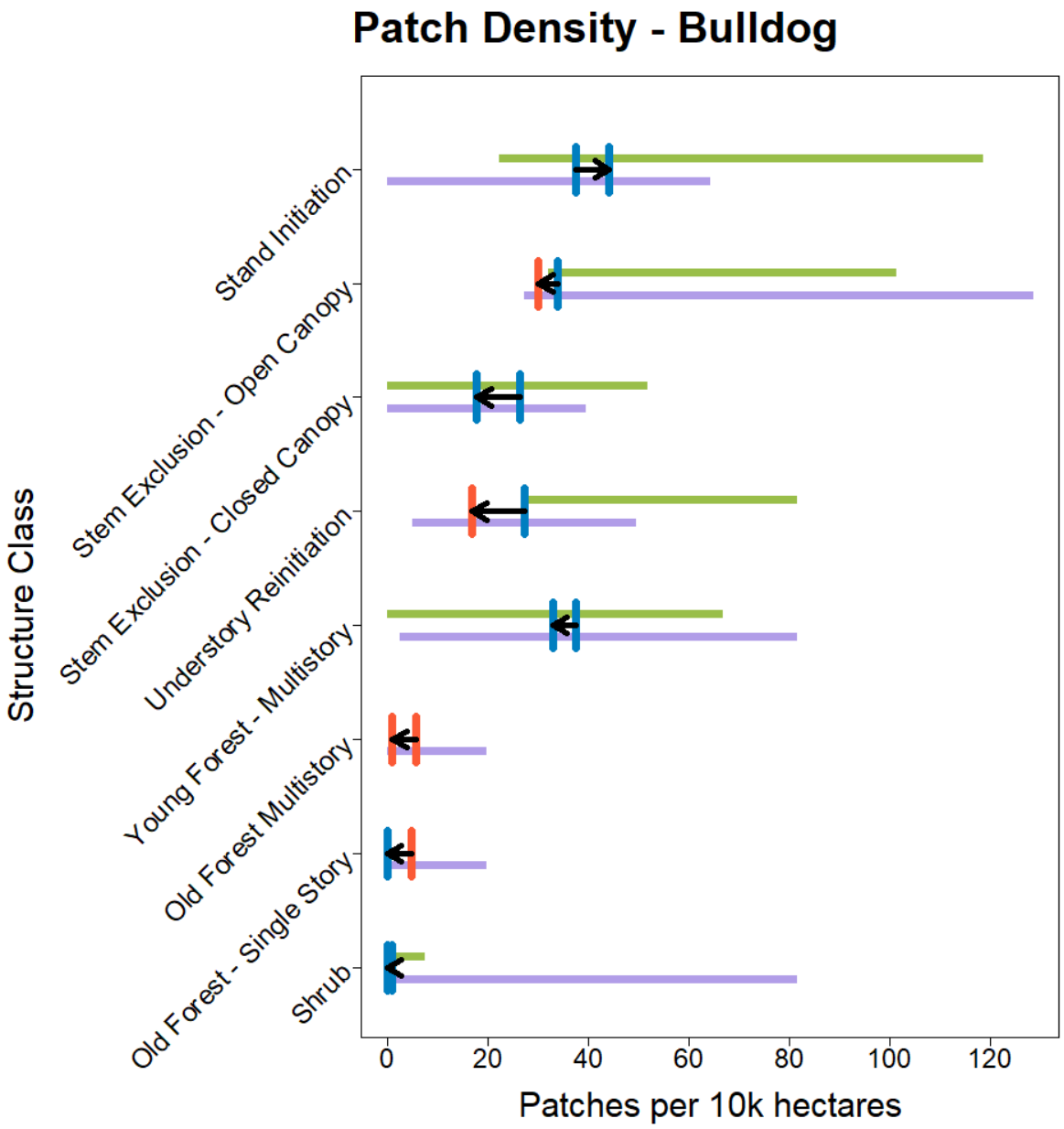

Figure 16. Midscale analysis of patch density for the Bulldog watershed using observed and predicted photo interpretation Structure Class. Green bars represent the range of conditions in the HRV dataset for the same ecological sub-region (ESR). Purple bars represent the range of conditions for the next warmest/driest ESR. Vertical bars represent the observed and predicted watershed scale values, with the arrow showing the direction of departure from the observed value. This figure shows how a land manager might identify aspects of watershed conditions departed from reference conditions and in need of restoration treatments.

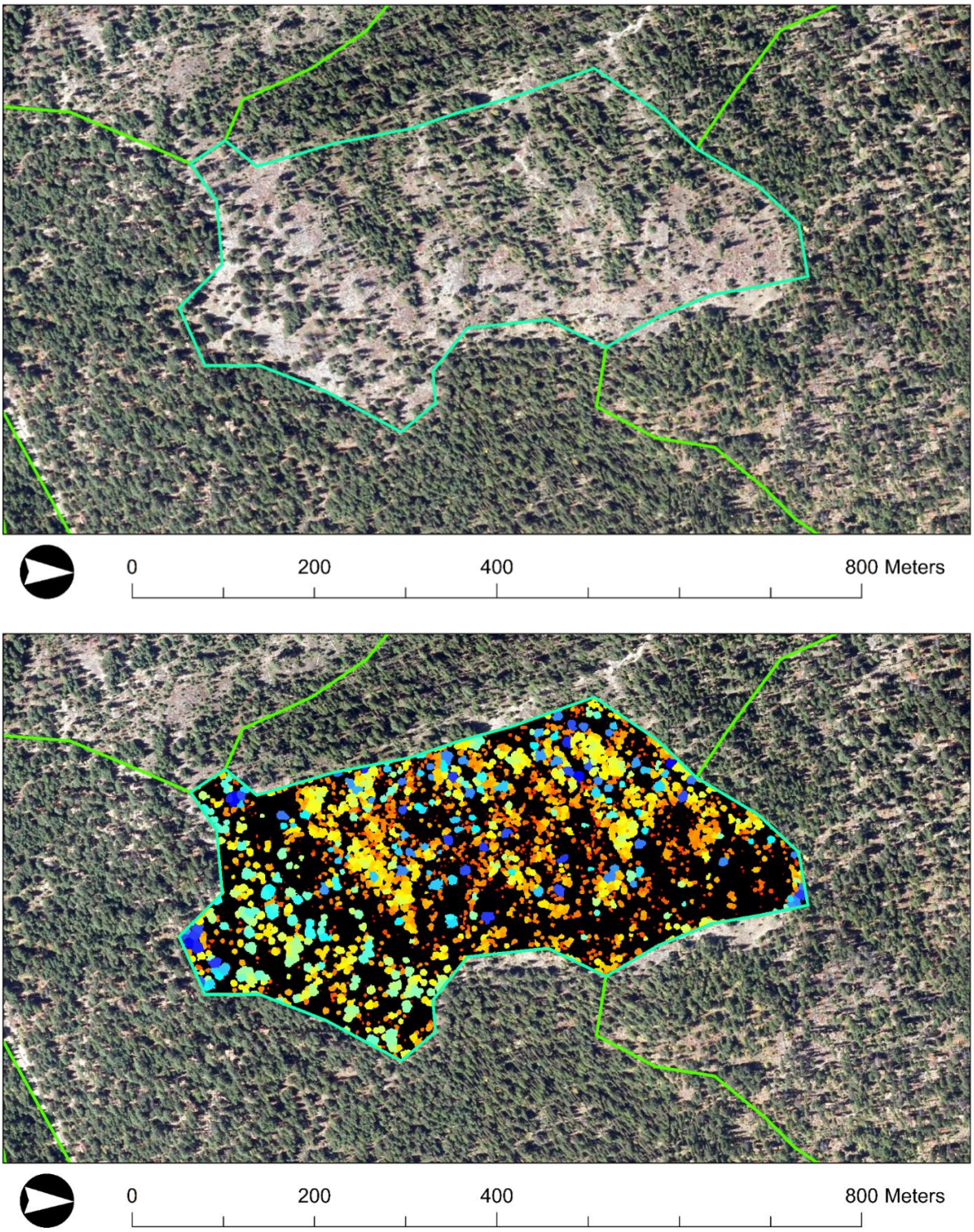

Figure 17. Comparison of orthoimagery (above) and Lidar derived TAO max height (below) for a single delineated patch. Cooler values in the Lidar data represent taller heights. Three distinct patterns are apparent in the Lidar data. While it is possible that these patterns could be identified using the orthoimagery alone, none of the three conditions occupies four hectares, which is the minimum size of a patch. This illustrates some of the challenges in predicting photo interpretation attributes using Lidar data.

9. Tables

Table 1. Photo interpretation attributes modeled in this study.

Attribute	Description	Values
Number of Canopy Strata	Number of distinct canopy layers visible from imagery	No canopy Layers Single canopy layer Two canopy layers More than two canopy layers
Total Canopy Cover	Percentage of patch area covered by canopy	0%, 10%, 20%, 30%, 40%, 50%, 60% 70%, 80%, 90%, 100%
Overstory Canopy Cover	Percentage of patch area covered by the canopy layer of the largest size class	0%, 10%, 20%, 30%, 40%, 50%, 60% 70%, 80%, 90%, 100%
Understory Canopy Cover	Total Canopy Cover minus Overstory Canopy Cover	0%, 10%, 20%, 30%, 40%, 50%, 60% 70%, 80%, 90%
Overstory Size Class	Average diameter at breast height of the most dominant canopy layer	No trees Seedling and Saplings (< 5”) Poles (5” to 8.9”) Small trees (9” to 15.9”) Medium trees (16” to 25”) Large trees (>25”)
Understory Size Class	Average diameter of the second most dominant canopy layer	Only Overstory Exists Seedling and Saplings (< 5”) Poles (5” to 8.9”) Small trees (9” to 15.9”) Medium trees (16” to 25”)
Structure Class	Descriptive metric describing vertical forest structure. Derived from a dichotomous key that considers Number of Canopy Strata and Overstory and Understory Canopy Cover and Size Class	Stand Initiation, Stem Exclusion - Open Canopy, Stem Exclusion - Closed Canopy, Understory Reinitiation, Young Forest - Multistory, Old Forest - Single Story, Old Forest - Multistory, Herb, Shrubs, Wood, Other
Simplified Canopy Cover	Total Canopy Cover reduced into fewer bins	>10%, 10%-30%, 40%-60%, >60%
Simplified Size Class	Single metric describing average tree size class	No Trees, Small, Medium, Large
Simplified Structure Class	Fewer binned structure class derived from simplified Canopy Cover and Size Class	Open, Small, Medium-Open, Medium, Medium-Closed, Large-Open, Large, Large-Closed, Very Large, Non-Forest

Table 2. Accuracy rate of Lidar driven predictive models of photo interpretation attributes. Values reported are for three way cross validated models using an a priori selection of predictor metrics. The single exception is Structure Class: Dichotomous Key, which was classified using predicted values.

Attribute	Accuracy			Kappa	
	Exact Match	Within One	Null	Exact Match	Within One
Number of Canopy Strata	0.62	0.99	0.60	0.21	0.98
Total Canopy Cover	0.31	0.77	0.20	0.21	0.74
Overstory Canopy Cover	0.22	0.54	0.16	0.11	0.47
Understory Canopy Cover	0.30	0.56	0.30	0.21	0.74
Overstory Size Class	0.47	0.92	0.42	0.19	0.88
Understory Size Class	0.47	0.81	0.36	0.23	0.74
Structure Class: Random Forest	0.39	NA	0.25	0.21	NA
Structure Class: Dichotomous Key	0.22	NA	0.25	0.001	NA
Simplified Canopy Cover	0.78	0.98	0.67	0.54	0.96
Simplified Size Class	0.59	0.98	0.52	0.31	0.97
Simplified Structure Class	0.57	NA	0.43	0.27	NA